

## Inhibition of Atmospheric Corrosion of Mild Steel by New Green Inhibitors under Vapour Phase Condition

Sudheer<sup>1</sup>, M. A. Quraishi<sup>1\*</sup>, Eno E. Ebenso<sup>2</sup>, M. Natesan<sup>3</sup>

<sup>1</sup> Department of Applied Chemistry, Indian Institute of Technology, (Banaras Hindu University) Varanasi -221 005, (India)

<sup>2</sup> Department of Chemistry, School of Mathematical and Physical Sciences, North-West University (Mafikeng Campus), Private Bag X2046, Mmabatho 2735, South Africa

<sup>3</sup> Central Electrochemical Research Institute Karaikudi -630 006, Tamilnadu, India

\*E-mail: [maquraishi.apc@itbhu.ac.in](mailto:maquraishi.apc@itbhu.ac.in); [maquraishi@rediffmail.com](mailto:maquraishi@rediffmail.com);

*Received:* 12 June 2012 / *Accepted:* 11 July 2012 / *Published:* 1 August 2012

---

Two new green volatile corrosion inhibitors namely oleic hydrazide benzoate (OHB) and oleic hydrazide salicylate (OHS) were synthesized. Their inhibition action was evaluated on corrosion of mild steel under a thin-film electrolyte consisting of simulated water using the weight loss, potentiodynamic polarization and electrochemical impedance methods. Atmospheric corrosion monitor cell (ACMC) was used to study the electrochemical properties of the inhibitors. The results of polarisation study show that OHB is anodic type and OHS is a mixed-type inhibitor. Oleic hydrazide benzoate (OHB) exhibited higher inhibition efficiency (89.31 % from potentiodynamic polarization ) under vapour phase condition.

---

**Keywords:** mild steel, atmospheric corrosion monitor cell, volatile corrosion inhibitors, EIS, atmospheric corrosion.

### 1. INTRODUCTION

The use of volatile corrosion inhibitors (VCIs) is one of the most effective and convenient methods for preventing corrosion of metals and equipments during storage and transportation [1-5]. Organic compounds having significant vapour pressure act as efficient inhibitors for corrosion under vapour phase condition even in presence of water vapour in the air [6, 7]. To evaluate the effectiveness of VCIs several techniques have been developed [8-12]. Rosenfeld [13] showed that the mechanism of this attack is electrochemical, in which the electrolyte is composed of a thin film of humidity on the surface of the metal. It has been shown for iron that when relative humidity is below 60 percent, no

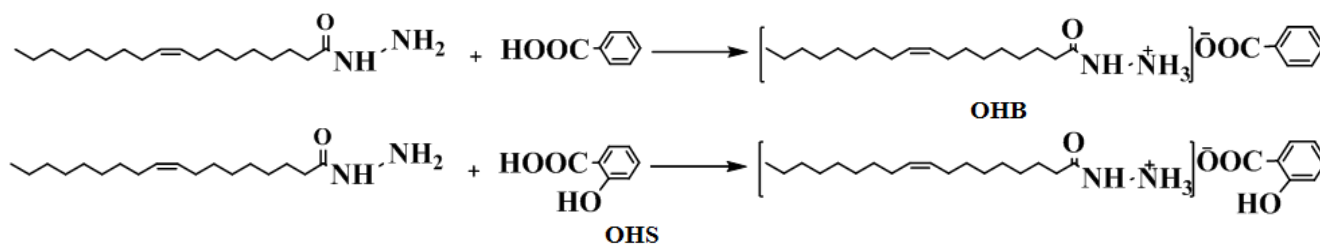
corrosion is expected, while above 75 percent, the degree of corrosion is high. The vapor of volatile corrosion inhibitors reach the metal surface and condense to form a thin film of crystals. In the presence of even traces of moisture, the crystal gets dissolved and immediately develops strong ionic activities. The layer separates the metal from the environment and protects the metal from corrosion [14].

The volatile corrosion inhibitor impregnated within wrapping material kraft paper may be used for packaging metallic objects. The salts may be impregnated in the wrappings by various means, such as, e.g. dissolving them (the inhibitors) in a relatively volatile solvent. There are numerous investigations on corrosion inhibition by organic compounds having heteroatoms and their salts as VCIs for various industrial metals alloys. The organic substances such as dicyclohexylamine [15], urea-amine [16], dicyclohexylamine nitrite [17], atmospheric amines [18], 1, 3-bis-diethyl aminopropan-2-ol [19], bis-piperidinium methyl urea [20] have been used as volatile corrosion inhibitors. Natural compounds like wood bark oil [21] and thyme [22] have also been used as VCIs. In continuation of our work [23-27], we report here synthesis and testing of the two new volatile corrosion inhibitors namely oleic hydrazide benzoate (OHB), and oleic hydrazide salicylate (OHS) on corrosion of mild steel under thin film of electrolyte containing 0.01 NaCl.

## 2. EXPERIMENTAL

### 2.1. Synthesis of Volatile Corrosion Inhibitors

The inhibitors were synthesized by dissolving one mole of the oleic hydrazide and one mole of corresponding organic acids in ethanol subsequently stirred for 20 minute at 40<sup>0</sup>C (Scheme 1.) The precipitated compounds were filtered and crystallized from ethanol and their melting points are OHB 100<sup>0</sup>C and OHS 105<sup>0</sup>C. The purity of the compounds was confirmed by thin layer chromatography.



**Scheme 1.** Synthetic route and structures of volatile corrosion inhibitors.

### 2.2. Material

Mild steel coupons of dimensions 2.5 cm x 2.0 cm x 0.025 cm were used for weight loss studies. The composition of mild steel by wt %: C 0.076%; Mn 0.192%; Si 0.026%; Cr 0.050%; P 0.012%; Cu 0.135%; Al 0.023%; Ni 0.05%; and balance Fe.

### 2.3. Accelerated Vapor Phase Corrosion Test Method

Weight loss measurements were made by specimens of mild steel having dimensions of 2.5 cm x 2.0 cm x 0.025 cm, and a hole was drilled in each for suspending the samples. These were abraded with emery paper of 600-1200 grades, washed thoroughly with doubled distilled water, degreased with acetone and finally dried. The experiments were carried out in the presence and absence of inhibitors at various concentrations (25, 50, 100 mg), by using tight fitting rubber cork jar's Fig. 1. These jars were kept at 90% relative humidity (RH) at 40°C in order to allow continuous condensation of moisture on the metal specimens [28, 29]. The mild steel specimens were level mounted on the top of the beaker by transparent adhesive, and just below these specimens vapor phase inhibitor samples were kept in a small bottle. This set up was kept for 14 days. The mill scale on the specimen was removed by using a suitable pickling solution, i.e., Clarke's solution (a mixture containing concentrated hydrochloric acid, 2% antimony trioxide (Sb<sub>2</sub>O<sub>3</sub>) and 5% stannous chloride (SnCl<sub>2</sub>)), washed, dried, and then weighed. All the experiments were performed in duplicate and average values are reported. The values of inhibition efficiency ( $\eta_{\%}$ ) and corrosion rate ( $r$ ) obtained at different concentrations of inhibitors are calculated from the weight loss data using the equation:

$$\eta_{\%} = \frac{w_0 - w_i}{w_0} \times 100 \quad (1)$$

where  $w_0$  and  $w_i$  are the weight loss value in the absence and presence of an inhibitor respectively. The corrosion rate ( $r$ ) in  $\text{mm} \cdot \text{y}^{-1}$  is determined by using the following equations:

$$r = \frac{87.6 \times w}{AtD} \quad (2)$$

where  $w$  is a weight loss of mild steel (mg),  $A$  the area of the coupon ( $\text{cm}^2$ ),  $t$  is the exposure time (h) and  $D$  the density of mild steel ( $\text{g cm}^{-3}$ ).

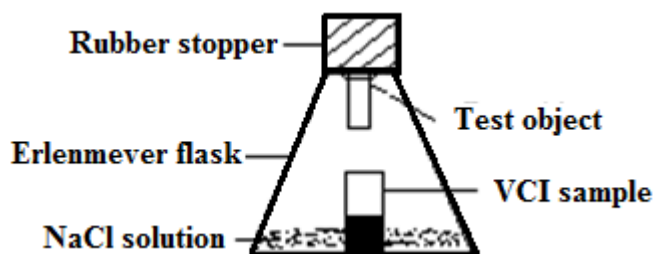


**Figure 1.** Experimental setup for weight loss method.

### 2.4. Preparation of impregnated Kraft paper

Volatile corrosion inhibitors (VCIs), oleic hydrazide benzoate (OHB), and oleic hydrazide salicylate (OHS) coated Kraft paper were prepared by using the impregnation method as described by

Subramanian et al. and Stroud et al. [29, 30]. A known amount of VCI was dissolved in a measured volume (25ml) of ethanol one sq. ft. of Kraft paper was dipped into the solution until completely wet and taken out; the solvent was allowed to evaporate. Then the weight of VCI impregnated kraft paper was noted and then stored in a tightly closed container, from which it was taken just before use.

### 2.5. Construction of the atmospheric corrosion monitor cell

Atmospheric corrosion monitoring cell (ACMC) having three electrodes was fabricated with respective metals [31, 13]. Atmospheric corrosion monitor was constructed by using five metal (mild steel) plates of size  $1 \times 0.5$  cm. The metal plates were insulated from one another by PVC separators of thickness 1mm. The central metal plate was connected to one terminal, which acted as the reference

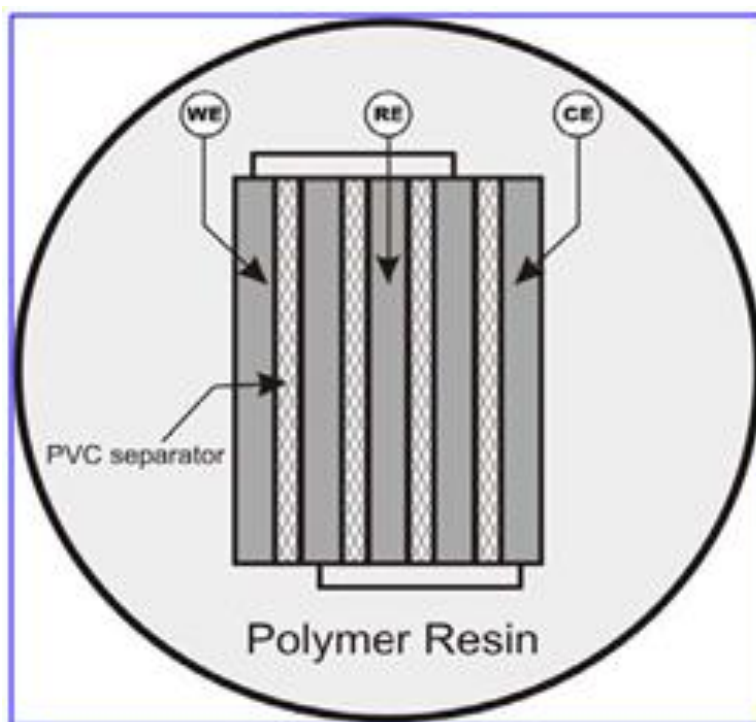


**Figure 2.** Atmospheric corrosion monitor cell.

electrode (RE). Two alternate plates (except central plate) were connected to two other terminals namely working electrode (WE) and counter electrode (CE). The whole setup was molded in polymeric resin to form atmospheric corrosion monitor as shown in Fig. 2.

### 2.6. Electrochemical measurements

The electrochemical studies were carried out using the three-electrode type atmospheric corrosion monitor cell with working electrode area of  $1 \text{ cm}^2$  cell assembly at  $40 \text{ }^\circ\text{C}$ . All

electrochemical measurements were carried out by thin layer technique using a Solatron model 1280B electrochemistry system with the computerized control system. The EIS measurements were performed in the frequency range of 10 KHz to 100 MHz

### 2.6.1. Potentiodynamic polarization measurements

Polarization measurements were determined potentiodynamically by thin layer technique for mild steel using the atmospheric corrosion monitor cell. One ml of the electrolyte (0.01N NaCl) was applied through a syringe on VCI treated (impregnated VCI's paper fixed on the ACMC electrode) paper on ACMC to form a thin film of electrolyte on the surface. The corrosion potential was first noted when the electrode attained a steady value. The potential was vary from cathodic to anodic direction from the corrosion potential and then the polarization measurements were carried out. The plot of  $E$  vs.  $\log I_{\text{corr}}$  was made from which corrosion potential ( $E_{\text{corr}}$ ), corrosion current density ( $I_{\text{corr}}$ ), anodic and cathodic Tafel slopes ( $\beta_a$  &  $\beta_b$ ) values are calculated. A similar experiment was carried out using unimpregnated kraft paper as control. The inhibition efficiency for these systems is calculated using the following equation [32, 33].

$$\eta_{\%} = \frac{I_{\text{corr}}^0 - I_{\text{corr}}^i}{I_{\text{corr}}^0} \times 100 \quad (3)$$

where,  $I_{\text{corr}}^0$  and  $I_{\text{corr}}^i$  are the corrosion current density using unimpregnated kraft paper and impregnated kraft paper, respectively.

### 2.6.2. Electrochemical impedance measurements

Electrochemical impedance measurements were determined for VCI impregnated and unimpregnated papers. One ml of 0.01N NaCl was applied on the well-polished three electrode type ACMC over which various concentrations of VCI impregnated papers were pressed and allowed to attain a steady potential value. The Nyquist plots give the values of charge transfer resistance. The inhibition efficiency ( $\eta_{\%}$ ) of the inhibitor are calculated by the charge transfer resistance values using the following equation: [34, 35]

$$\eta_{\%} = \frac{R_{\text{ct}}^i - R_{\text{ct}}^0}{R_{\text{ct}}^i} \times 100 \quad (4)$$

where,  $R_{\text{ct}}^0$  and  $R_{\text{ct}}^i$  are the charge transfer resistance in absence and in the presence of an inhibitor, respectively.

### 3. RESULTS AND DISCUSSION

#### 3.1. Accelerated Vapor Phase Corrosion Test

The weight loss measurement for mild steel in the absence and the presence of varying concentrations of inhibitors under 90% RH at 40<sup>0</sup>C for the period of 14 days is summarized in Table 1. From the weight loss, inhibition efficiency ( $\eta_{\%}$ ) and corrosion rate ( $r$ ,  $\text{mm y}^{-1}$ ) are calculated as described. Visual inspection is the criterion for the vapor phase corrosion inhibition test. It is observed that whole part of the metal specimens was severely affected by atmospheric corrosion and less affected in presence of VCI shown in Fig. 3. The better inhibition efficiency at a higher concentration may be due to larger coverage of metal with inhibitor molecules. Both VCIs showed good inhibition efficiencies, 89.97 % which may be attributed to the formation of a good physical barrier between metal and corrosive environment by the interaction of metal and VCIs.

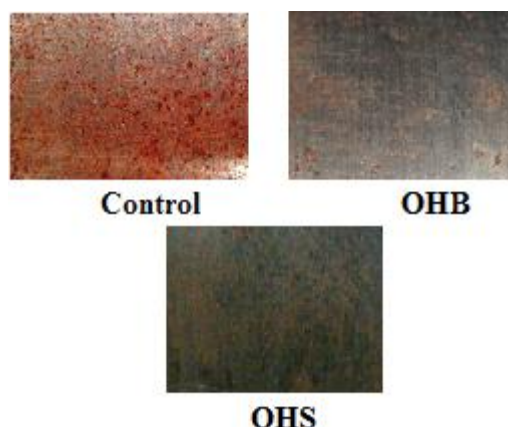


**Figure 3.** Visual inspection of metal specimens.

**Table 1.** Weight loss, inhibition efficiency, and corrosion rate parameter obtained by weight loss measurements from OHB, and OHS VCI at 40<sup>0</sup>C and 90% relative humidity for 14 days, for mild steel.

| Concentration of Inhibitor (mg) | Weight loss (mg cm <sup>-2</sup> ) | Corrosion rate (mm y <sup>-1</sup> ) | Inhibition efficiency |
|---------------------------------|------------------------------------|--------------------------------------|-----------------------|
| Control                         | 41.9                               | 0.1384                               | -                     |
| OHB                             |                                    |                                      |                       |
| 25                              | 19.2                               | 0.0634                               | 54.18                 |
| 50                              | 8.5                                | 0.0280                               | 79.71                 |
| 100                             | 4.2                                | 0.0138                               | 89.97                 |
| OHS                             |                                    |                                      |                       |
| 25                              | 19.2                               | 0.0634                               | 50.84                 |
| 50                              | 10.8                               | 0.0356                               | 74.22                 |
| 100                             | 4.2                                | 0.0138                               | 89.97                 |

3.2 Electrochemical measurements

3.2.1. Potentiodynamic Polarization Measurements

Polarization measurements were performed in order to gain knowledge concerning the kinetics of the cathodic and anodic reactions. Fig. 4 (a, b) represents the potentiodynamic polarization curves in 0.01N NaCl at different concentrations of OHB, and OHS treated paper and untreated papers on the mild steel electrode. The various electrochemical parameters such as corrosion potential ( $E_{corr}$ ), corrosion current density ( $I_{corr}$ ), anodic and cathodic Tafel slopes ( $\beta_a$  and  $\beta_c$ ) are given in Table 2. The linear Tafel segments of anodic and cathodic curves were extrapolated to corrosion potential to obtain corrosion current densities ( $I_{corr}$ ) [36, 37]. In the present study, from the Tafel polarization curves – Fig. 4 (a-b), show that at optimum concentration of OHB there is a shift of  $E_{corr}$  values in the positive direction while OHS does not cause significant shift of  $E_{corr}$ . So it is suggested that OHB inhibit the corrosion predominately as an anodic type inhibitor and OHS act as mixed-type inhibitor [38].

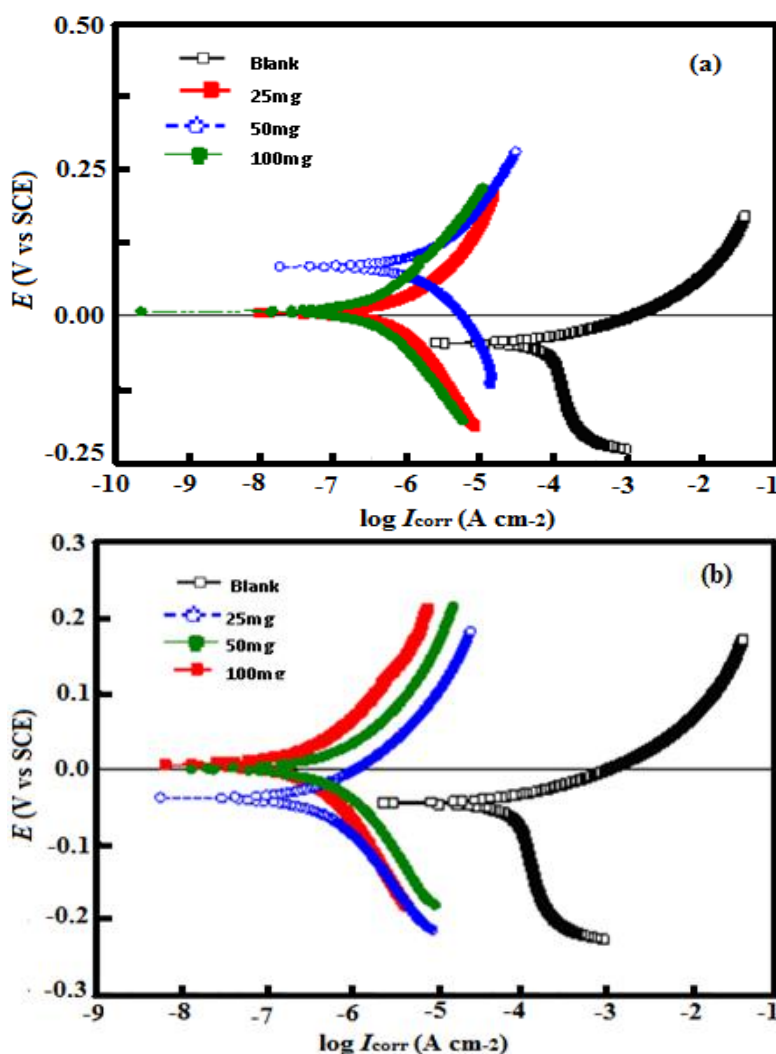


**Figure 4.** Potentiodynamic polarization curves for mild steel wrapped with different concentration (a) OHB (b) OHS VCIs impregnated paper in 0.01N NaCl by thin layer technique.

It is also seen from the Table 2 that corrosion current ( $I_{\text{corr}}$ ) decreases in the presence both inhibitors. OHB and OHS showed 98.31 % and 97.39 % inhibition efficiency at 100 mg/ft<sup>2</sup> concentration.

**Table 2.** Potentiodynamic polarization parameters for mild steel with OHB, and OHS, VCI impregnated and unimpregnated paper in 0.01N NaCl by thin layer technique.

| Concentration of VCI (mg/ft <sup>2</sup> ) | $E_{\text{corr}}$ (mV) | Tafel slopes (mV/decade) |     | $I_{\text{corr}}$ ( $\mu\text{A}/\text{cm}^2$ ) | Inhibition efficiency (%) |
|--|------------------------|--------------------------|-----|---|---------------------------|
|  |                        | ba                       | -bc |   |                           |
| Blank                                      | -60.10                 | 54                       | 270 | 84.73   | -                         |
| OHB  |                        |                          |     |   |                           |
| 25   | 0.84                   | 129                      | 187 | 2.54  | 97.00                     |
| 50   | 65.25                  | 112                      | 200 | 1.84  | 97.80                     |
| 100  | 45.84                  | 146                      | 161 | 1.43  | 98.31                     |
| OHS  |                        |                          |     |   |                           |
| 25   | -38.86                 | 112                      | 189 | 7.27  | 91.41                     |
| 50   | 4.25                   | 159                      | 125 | 2.49  | 97.06                     |
| 100  | -0.58                  | 139                      | 198 | 2.21  | 97.39                     |

### 3.2.2. Electrochemical Impedance Measurements

The impedance spectra of volatile corrosion inhibitors OHB and OHS treated paper and untreated papers on the mild steel electrode at the different concentrations are depicted in Fig. 5 (a, b). Electrochemical impedance measurements were carried over the frequency range from 10 kHz to 100 MHz at open circuit potential by using a Solatron model 1280B system with computerized control. The sinusoidal potential perturbation was 5 mV in amplitude. The solution resistance ( $R_s$ ) and total resistance ( $R_t$ ) were obtained from the low frequency and high-frequency intercepts on  $Z_{\text{real}}$ -axis of Nyquist's plot respectively. The difference between  $R_t$  and  $R_s$  values gives the charge transfer resistance ( $R_{\text{ct}}$ ) value. The Nyquist's plots Fig. 5 (a, b) were similar to a depressed semicircle, which was a typical behavior for solid electrodes that showed frequency dispersion of the impedance data [39, 40]. A general equivalent circuit model used to analyze the EIS data of mild steel with VCIs is shown in Fig. 6. The impedance parameters obtained from the curves are given in Table 3. The  $C_{\text{dl}}$  values were obtained from the equation.

$$C_{\text{dl}} = \frac{1}{2\pi f_{\text{max}} R_{\text{ct}}} \quad (5)$$

where  $C_{\text{dl}}$  - double layer capacitance,  $R_{\text{ct}}$  - charge transfer resistance,  $f_{\text{max}}$  - frequency at  $Z''$  value maximum. It can see from Table 3 the  $R_{\text{ct}}$  values increases with increasing in the concentration of the inhibitor. The increase in  $R_{\text{ct}}$  value is attributed to the formation of protective film on the metal/solution interface. This indicated that a charge transfer process mainly control the corrosion

process [41]. On the other hand the value of  $C_{dl}$  decreases with increases in the inhibitor concentration. The double layer between the charged metal surface and the solution is considered as an electrical capacitor. This decrease in  $C_{dl}$  results from a decrease in local dielectric constant and/or an increase in the thickness of the double layer, suggested that inhibitor molecules inhibit the iron corrosion by adsorption at the metal/acid interface [42].

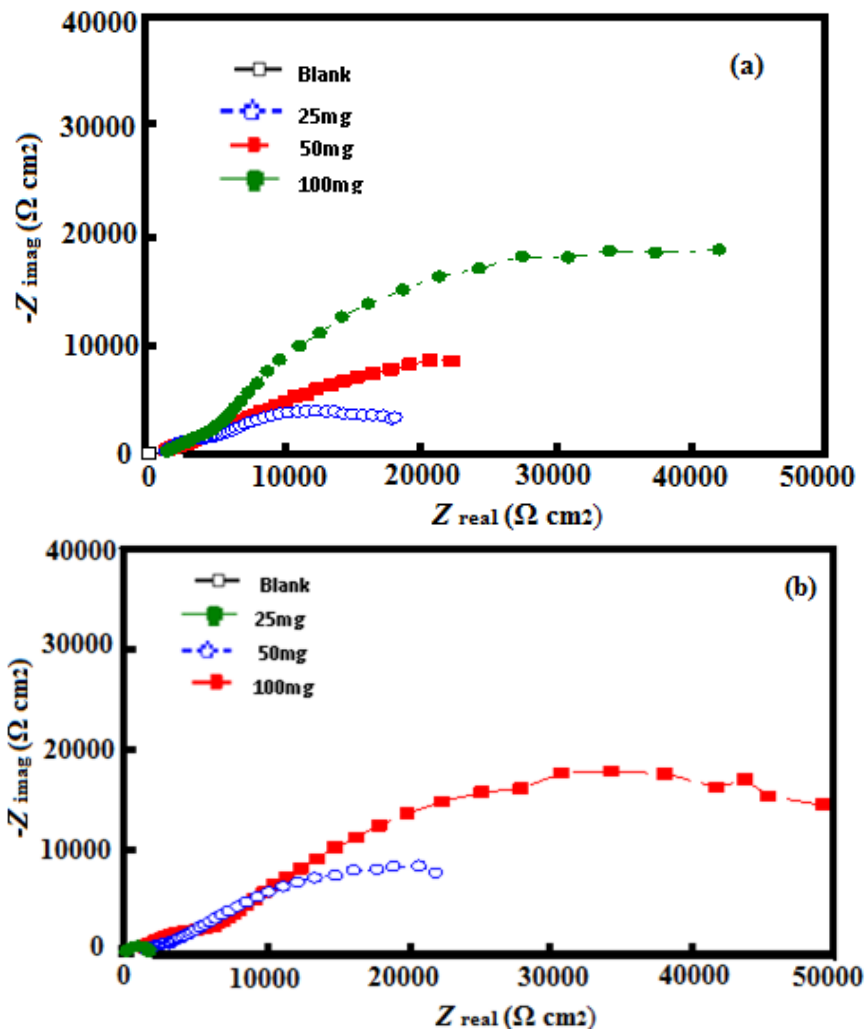


**Figure 5.** AC Impedance curves for mild steel wrapped with (a) OHB (b) OHS VCIs impregnated paper in 0.01N NaCl by thin layer technique.

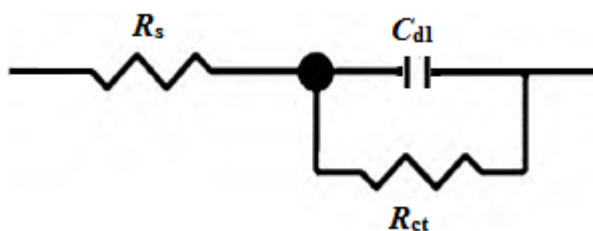


**Figure 6.** Equivalent circuit model used to analyze the electrical behavior of mild steel.

**Table 3.** AC Impedance parameters for mild steel with OHB, and OHS VCI impregnated and unimpregnated paper in 0.01N NaCl by thin layer technique.

| Concentration of VCI (mg/ft <sup>2</sup> ) | R <sub>ct</sub> (k.ohm cm <sup>2</sup> ) | C <sub>dl</sub> (μF/cm <sup>2</sup> ) | Inhibition efficiency (%) |
|--|--|---------------------------------------|---------------------------|
| Blank OHB                                  | 7.34                                     | 0.434                                 | -                         |
| 25   | 20.03                                    | 0.1590                                | 63.36                     |
| 50   | 63.62                                    | 0.0455                                | 88.46                     |
| 100 OHS                                    | 66.67                                    | 0.0434                                | 88.99                     |
| 25   | 17.32                                    | 0.2660                                | 57.62                     |
| 50   | 38.50                                    | 0.0858                                | 80.93                     |
| 100  | 59.31                                    | -                                     | 87.62                     |

It is shown from the impedance results that the VCIs inhibit the corrosion of mild steel in 0.01 N, NaCl solutions and the inhibition efficiency increases by increasing the concentration on kraft paper Table 3. The AC impedance method of evaluation corroborates the results obtained from gravimetric and polarization studies.

### 3.3. Adsorption Isotherm

It is widely acknowledged that adsorption isotherms provide useful insights into the mechanism of corrosion inhibition. The adsorption isotherm study describes the interaction between inhibitor molecules and mild steel surface. The values of surface coverage ( $\theta$ ) at different inhibitor concentrations were evaluated from weight loss values. Different adsorption isotherms were tested in order to find the best suitable adsorption isotherm for adsorption of VCIs on the surface of mild steel from 0.01 N NaCl solution. Langmuir adsorption isotherm was found to be best fit according to following equation: [43]

$$\frac{\theta}{1-\theta} = kC \exp(-\Delta G_{\text{ads}} / RT) \quad (6)$$

where  $\Delta G_{\text{ads}}$  is free energy of adsorption, R is gas constant, and T is temperature in K. A straight line was obtained on plotting  $\log(\theta/1-\theta)$  versus  $\log C$  (concentration) Fig. 7.

### 3.4. Mechanism of Corrosion Inhibition

The results obtained from different electrochemical and weight loss measurements reveal that both the volatile corrosion inhibitors (OHB and OHS) inhibit the corrosion of mild steel in 0.01 NaCl by adsorption. Mechanism of VCIs inhibits corrosion of metal in the following ways;

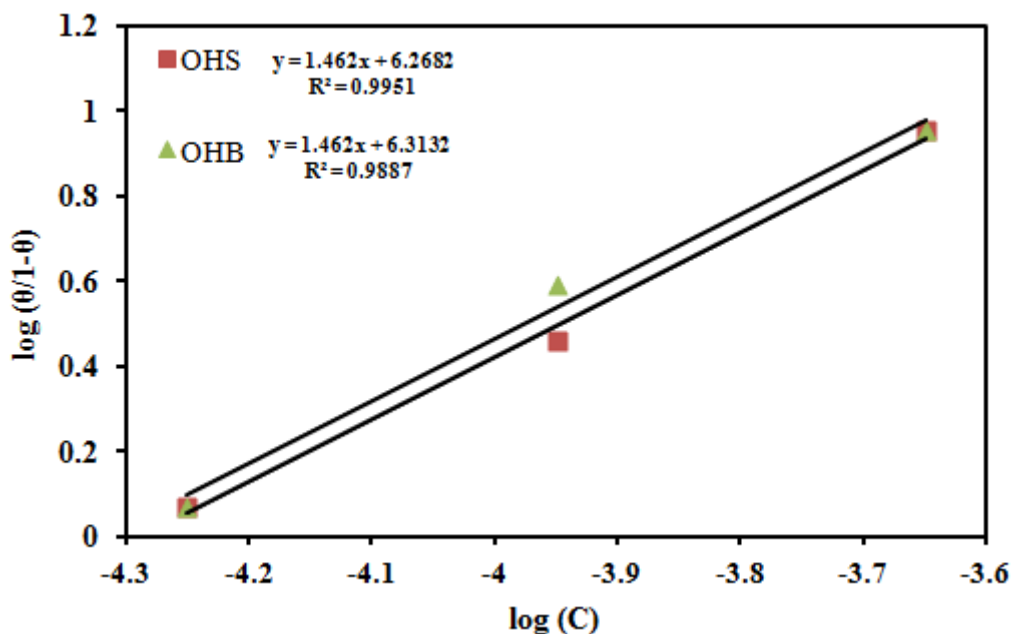


**Figure 7.** Langmuir adsorption isotherm plots for VCIs on mild steel.

- (i). By saturating the space with their vapours and reducing the relative humidity below the critical value [44].
- (ii). By alkalizing the medium to pH values at which the rate of corrosion becomes significantly low [45].
- (iii). By producing a high ohmic resistance on the metal surface which reduces the corrosion current to a minimum value [46].
- (iv). By rendering the metal surface hydrophobic thereby preventing the reaction of the metal with the environment [47].

The inhibition of metallic corrosion in the presence of VCIs involves vaporization of the inhibitor in a non-dissociated molecular form, followed by hydrolysis of the salts into the carboxylate anion and oleate hydrazide cation. Anion is adsorbed on the anodic site of the metal and inhibits anodic reaction, while organic cation is adsorbed on the cathodic side, thereby preventing cathodic reaction [38].

#### 4. CONCLUSIONS

Both the volatile corrosion inhibitor namely OHB and OHS have been found to be effective corrosion inhibitors for mild steel under vapour phase condition. The inhibitive performance of both VCI increases on increasing the inhibitor concentration. OHB exhibited better performance as VCI than the OHS for mild steel. The results of polarisation study showed that OHB is anodic and OHS is mixed type inhibitor. The adsorption of the inhibitors on the metal surface followed the Langmuir adsorption isotherm. The VCI molecules render the metal surface hydrophobic and thus prevent the reaction of metal with the environment.

## ACKNOWLEDGMENT

One of the authors, Sudheer is thankful to University Grant Commission (UGC), New Delhi, India for the financial assistance from UGC (RFSMS).

## References

1. C. Leygraf, and T. E. Graedel, *Atmospheric corrosion*, Wiley, (2000)
2. A. Subramanian, M. Natesan, V. S. Muralidharan, K. Balakrishnan and T. Vasudevan, *Corrosion*, 56 (2000) 144
3. D. M. Bastidas, E. Cano and E. M. Mora, *Anti.corros. Methods Mater*, 52 (2005) 71
4. D. Q. Zhang and L. X. Gao, *Mater. Perform.*, 42 (2003) 40
5. W. A. McKay, J. A. Garland, D. Livesley, C. M. Halliwell and M. I. Walker, *Atmos. Environ.*, 28 (1994) 3299
6. V. S. Sastri, E. Ghali and M. Elboudjaini, *Corrosion Prevention and Protection Practical Solutions*, John Wiley & Sons, England (2007)
7. M. G. Fontana, *Corrosion Engineering*, Mc Graw-Hill International, New York (1987)
8. E. G. Stroud and W. H. J. Vernon, *J. of Appl. Chem.*, 2 (1952) 166
9. I. L. Rosenfeld, V. P. Persiantseva, G. G. Samoilenko and Y.N. Mudzhiri, *Zashch. Met.*, 18 (1982) 484
10. F. Mansfeld and S. Tsai, *Corros. Sci.*, 20 (1980) 853
11. A. wachter, T. Skei and N. Stillmn, *Corrosion*, 7 (1951) 284
12. E.I. Kozlova and V. L. Mironov, *Zashch. Met.* 20 (1984) 966
13. I. L. Rosenfeld, *Proceedings of the First International Congress on Metallic Corrosion*, Butterworth, London (1962)
14. W. Skinner, F. du Preez and E. Vuorinen, *Brit. Corros. J.*, 34 (1999) 151
15. A. Subramanian, P. Rajendran, M. Natesan, K. Balakrishnan and T. Vasudevan, *Anti.-corros. Methods Mater.*, 46 (1999) 346
16. D. Q. Zhang, L. X. Gao and G. D. Zhou, *Surf. Coat. Tech.*, 204 (2010) 1646
17. E. Cano, D. M. Bastidas, J. Simancas and J. M. Bastidas, *Corrosion.*, 61 (2005) 473
18. X. Ge, A. S. Wexler and S. L. Clegg, *Atmos. Environ.*, 45 (2011) 524
19. G. Gao and C. H. Liang, *Corros. Sci.*, 49 (2007) 3479
20. D. Q. Zhang, Z. X. An and Q. Y. Pan, *Corros. Sci.*, 48 (2006) 1437
21. N. Poongothai, P. Rajendran, M. Natesan and N. Palaniswamy, *Indian J. Chem. Techn.*, 12 (2005) 641
22. P. Premkumar, K. Kannan and M. Natesan, *J. Metall. Mater. Sci.*, 50 (2008) 227
23. M. A. Quraishi<sup>1</sup>, F. A. Ansari and J. Rawat, *T O Elec. J.*, 1 (2009) 32
24. M. A. Quraishi, V. Bhardwaj and D. Jamal, *Bull. Electrochem.*, 19 (2003) 295
25. M. A. Quraishi, V. Bhardwaj and D. Jamal, *Indian J. Chem. Techn.*, 12 (2005) 93
26. M. A. Quraishi and D. Jamal, *J. Metall. Mater. Sci.*, 47 (2005) 45
27. M. A. Quraishi and F. A. Ansari, *Chem. Eng. Comm.*, 198 (2011) 1
28. I. L. Rosenfeld, V. P. Persiantseva and P. B. Terentiev, *Corrosion.*, 7 (1964) 222
29. A. Subramanian, Ph.D. Thesis, Alagappa University, Karaikudi, India (1998)
30. E. G. Stroud and W. H. I. Vernon, *J. of Appl. Chem.*, 2 (1952) 166
31. A. Subramanian, M. Natesan, A. Gopalan, K. Balakrishnan and T. Vasudevan, *Bull. Of Electrochem.* , 15 (1999) 54
32. A. K. Singh, E. E. Ebenso, and M. A. Quraishi, *Int. J. Electrochem. Sci.*, 7 (2012) 2320
33. I.B. Obot, E.E. Ebenso, I. A. Akpan<sup>1</sup>, Z. M. Gasem, and Ayo S. Afolabi, *Int. J. Electrochem. Sci.*, 7 (2012) 1978
34. S. K. Shukla, M. A. Quraishi and E. E. Ebenso, *Int. J. Electrochem. Sci.*, 6 (2011) 2912

35. A. K. Singh, and M. A. Quraishi, *Corros. Sci.*, 53 (2011) 1288
36. W. Skinner, *Corros. Sci.*, 35 (1993) 1491
37. P.C. Okafor, M.E. Ikpi, I. E. Uwah, E. E. Ebenso, U. J. Ekpe, and S. A. Umoren, *Corros. Sci.* 50 (2008) 2310
38. Y. Zou, J. Wang and Y. Y. Zheng, *Corros. Sci.*, 53 (2011) 208
39. M. Behzadnasab, S. M. Mirabedini, K. Kabiri and S. Jamali, *Corros. Sci.*, 53 (2011) 89
40. I. Ahamad, R. Prasad, M. A. Quraishi, *Corros. Sci.* 52 (2010) 933
41. A.K. Singh, M. A. Quraishi, *Corros. Sci.* 52 (2010) 152
42. A. Subramanian, K. R. Rathina, M. Natesan and T. Vasudevan, *Anti.-corros. Methods Mater.*, 49 (2002) 354
43. M. A. Quraishi, and S. K. Shukla, *Mater. Chem. Phys.* 113 (2009) 685-689
44. O. I. Golianitsky, *Volatile Inhibitors of Atmospheric Corrosion of Ferrous Metals*, Cheliabinsk Publishers (1958)
45. H. R. Backer, *Ind. Eng. Chem.*, 46 (1954) 2542
46. Kohler and Braun, *Combustion*, 25 (1954) 55
47. N. Hackerman, and J. D. Sudbury 97 *J. Electrochem. Soc.*, 97 (1950) 109